Module 5: Schlieren and Shadowgraph
Lecture 26: Introduction to schlieren and shadowgraph

The Lecture Contains:

- Introduction
- Laser Schlieren
  - Window Correction
- Shadowgraph

  - Shadowgraph
  - Governing Equation and Approximation
  - Numerical Solution of the Poisson Equation
  - Ray tracing through the KDP solution: Importance of the higher-order effects
  - Correction Factor for Refraction at the glass-air interface
  - Methodology for determining the supersaturation at each stage of the Experiment

Introduction

Closely related to the method of interferometry are $Schlieren$ and $Shadowgraph$ that employ variation in refractive index with density (and hence, temperature and concentration) to map a thermal or a species concentration field. With some changes, the flow field can itself be mapped. While image formation in interferometry is based on changes in the the refractive index n with respect to a reference domain, schlieren uses the transverse derivative $\partial n/\partial y$ for image formation. In shadowgraph, effectively the second derivative $\partial^2 n/\partial y^2$ (and in effect the Laplacian $\nabla^2 n$) is utilized. These two methods use only a single beam of light. They find applications in combustion problems and high-speed flows involving shocks where the gradients in the refractive index are large. The schlieren method relies on beam refraction towards zones of higher refractive index. The shadowgraph method uses the change in light intensity due to beam expansion to describe the thermal/concentration field.

Before describing the two methods in further detail, a comparison of interferometry (I), schlieren (Sch) and shadowgraph (Sgh) is first presented. The basis of this comparison will become clear when further details of the measurement procedures are described.

1. Interferometry relies on the changes in the refractive index in the physical region and hence the changes in the optical path length relative to a known (reference) region. Schlieren measures the small angle of deflection of the light beam as it emerges from the test section. Shadowgraph measures deflection as well as displacement of the light beam at the exit plane of the apparatus.

2. Displacement effects of the light beam are neglected in schlieren while displacement as well as deflection effects are neglected in interferometry. In effect, the light rays are taken to travel straight during interferometry.

3. Since large gradients will displace and deflect the light beams, interferometry is suitable for small gradients and shadowgraph for very large gradients. Schlieren fits well in the intermediate range.

4. In a broad sense, interferometry yields the refractive index field $n(x,y)$, schlieren - the gradient field ∇n and shadowgraph $-\nabla^2 n$.

5. Since deflection and displacement calculations are more complicated than that of the optical path length, shadowgraph analysis is the most involved, schlieren is less so, and interferometry is the simplest of the three.

6. All the three methods yield a cumulative information of the refractive index field (or its gradients), integrated in the viewing direction, i.e. along the path of the light beam.

7. As will be seen in the text of this module, schlieren and shadowgraph methods require simpler optics than interferometry. Shadowgraph is the simplest of all. The price to be paid is in terms of the level (and complexity) of analysis.
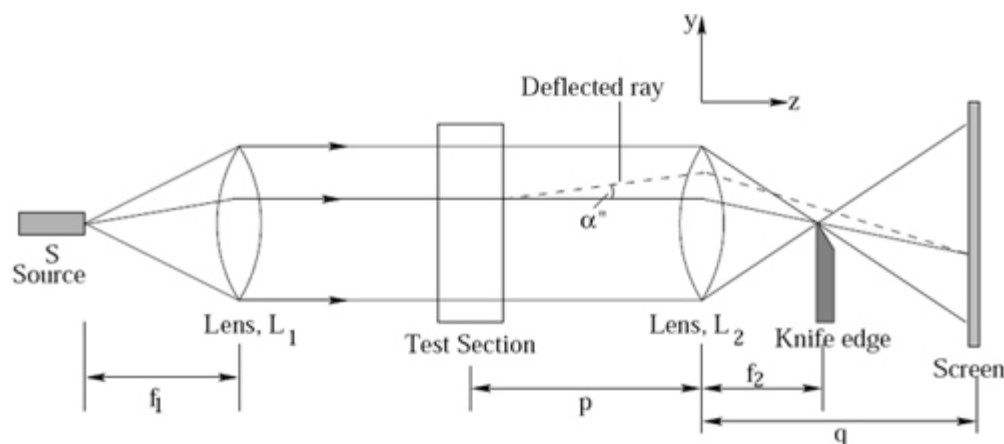
Figure 5.1: A schematic drawing of the schlieren set-up.

A schematic drawing of the schlieren layout is shown in Figure 5.1. In the arrangement shown, lens L_1 produces a parallel beam that passes through the test cell TC. Density gradients arising from temperature gradients in the test cell lead to beam deflection shown by dashed lines 1 and 2 in the figure above. A discussion on this subject is available in the context of refraction errors in interferometry.

A key element in the schlieren arrangement is the knife edge. It is an opaque sheet with a sharp edge. The deflected light beam emerging from the test cell is decollimated using a lens or a concave mirror. If the light spot moves downwards, it is blocked by the knife edge and the screen is darkened. If the light spot moves up, a greater quantity of light falls on the screen and is suitably illuminated. Thus, the knife edge serves as a *cut-off* filter for intensity. An appropriate term that characterizes this process is called *contrast*, measured as the ratio of change in intensity at a point and the initial intensity prevailing at that location. The knife edge can be seen as an element that controls contrast in light intensity. The change in contrast depends on the initial blockage and hence the initial intensity distribution on the screen. If the initial (undeflected) light beam is completely cut-off by the knife edge, the screen would be dark. Any subsequent beam deflection would illuminate the screen, thus producing a significant increase in contrast.

In Figure 5.1, the knife edge is kept at the focus of the lens L_2 and the screen at the conjugate focus of the test cell. In other words, the distances $p, q, and\ f_2$ satisfy the relation

$$\frac{1}{p} + \frac{1}{q} = \frac{1}{f_2}$$

In Figure 5.1, ray 1 increases the illumination at a point P on the screen while ray 2 is blocked by the knife edge and this results in a reduction in the illumination. Hence the image of the scaler field is seen as a distribution of intensities on the screen.

Previous   Next

In a schlieren measurement, beam displacement normal to the knife edge will translate into an intensity variation on the screen. Displacements that are blocked by the knife edge sheet are not recorded. Similarly, displacements parallel to the knife edge will also not change the intensity distribution. Information about these gradients in the respective directions can be retrieved by suitably orienting the knife edge. Other strategies such as using a gray scale filter are available. A color filter leading to a *color schlieren* measurement is desrcibed later in this module.

Consider the displacement of ray 1 as in Figure 5.2. At point P the illumination is proportional to a, say, equal to $k \times a$. With the test cell in place this becomes $k(a + \Delta a)$. Hence at P the contrast with respect to the undisturbed region is proportional to $\Delta a / a$. The contrast increases greatly when the initial illumination a is small, but it can lead to difficulties in recording the schlieren pattern. It can be shown that

$$\Delta a \approx f_2 \times p$$

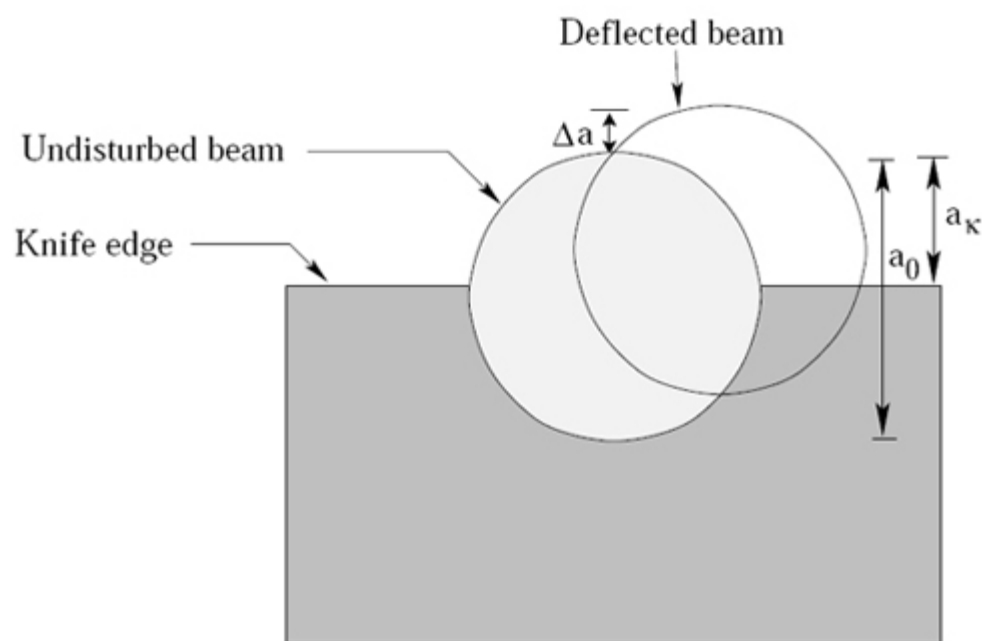and the contrast can be adjusted using the focal length of lens L_2.

Figure 5.2: Initial and final positions of the light spot with respect the knife edge.

Laser Schlieren

Image formation in a schlieren system is due to the deflection of light beam in a variable refractive index field towards regions that have a higher refractive index. In order to recover quantitative information from a schlieren image, one has to determine the cumulative angle of refraction of the light beam emerging from the test cell as a function of position in the $x - y$ plane. This plane is defined to be normal to the light beam, whose direction of propagation is along the z −coordinate. The path of the light beam in a medium whose index of refraction varies in the vertical direction (y) can be analyzed using the principles of geometric or rays optics as follows:

Consider two wave fronts at times τ and $\tau + \Delta\tau$ as shown in Figure 5.3. At time τ the ray is at a position z. After a interval $\Delta\tau$, the light has moved a distance of $\Delta\tau$ times the velocity of light, which in general, is a function of y, and the wave front or light beam has turned an angle $\Delta\alpha$. The local value of the speed of light is c_0/n where c_0 is the velocity of light in vaccum and n is the refractive index of the medium. Hence the distance Δz that the light beam travels during time interval $\Delta\tau$ is

$$\Delta z = \Delta\tau \, \frac{c_0}{n}$$

There is a gradient in the refractive index along the y direction. The gradient in n results in a bending the wave front due to refraction. The distance $\Delta^2 z$ is given by

$$\Delta^2 z = \Delta z_y - \Delta z_{y+\Delta y} \approx \Delta z_y - \Delta z_y - \frac{\Delta}{\Delta y}\,(\Delta z)\,(\Delta y) = -c_0 \, \frac{\Delta(1/n)}{\Delta y}\,\Delta\tau\,\Delta y$$

Let $\Delta\alpha$ represent the blending angle at a fixed location z. For a small increment in the angle, $\Delta\alpha$ can be expressed as

$$\Delta\alpha = \tan(\Delta\alpha) = \frac{\Delta^2 z}{\Delta y} = -c_0 \, \frac{\Delta\,(1/n)}{\Delta y}\,\Delta\tau = -n\Delta z \, \frac{\Delta\,(1/n)}{\Delta y}$$

In the limiting case

$$d\alpha = \frac{\partial(\ln n)}{\partial y}\,dz \qquad\qquad\qquad \textbf{(1)}$$

Hence the cumulative angle of the light beam at the exit of the test region will be given by

$$\alpha = \int \frac{\partial(\ln n)}{\partial y}\,dz \qquad\qquad\qquad \textbf{(2)}$$

where the integration is performed over the entire length of the test region.

◀‖ Previous   Next ‖▶

If the refractive index within the test section is different from that of the ambient air n_a, then from Snell's law, the angle of the light beam α'' after it has passed through the test section and emerged into the surrounding air is given by

$$n_a \sin\alpha'' = n \sin\alpha$$

For small values of α and α'',

$$\alpha'' = \frac{n}{n_a} \alpha$$

Therefore, Equation 2 gives

$$\alpha'' = \frac{n}{n_a} \int \frac{\partial(l_n n)}{\partial y} dz$$

If the factor $1/n$ within the integrand does not change greatly through the test section, then

$$\alpha'' = \frac{n}{n_a} \int \frac{\partial(l_n n)}{\partial y} dz$$

Let L be the length of the test section along the direction of the propogation of the light beam. Since $n_a \approx 1.0$ the cumulative angle of refraction of the light beam emerging into the surrounding air is given by

$$\alpha'' = \int_0^L \frac{\partial n}{\partial y} dz \qquad (3)$$

A schlieren system is basically a device to measure the angle α, typically of the order of $10^{-6} - 10^{-3}$ rad, as a function of position in the x-y plane normal to the light beam. Consider the system shown in Figure 5.3. A light source with dimensions $a_s \times b_s$ is kept at the focus of lens L_1 and provides a parrallel beam of light which probes the test section.
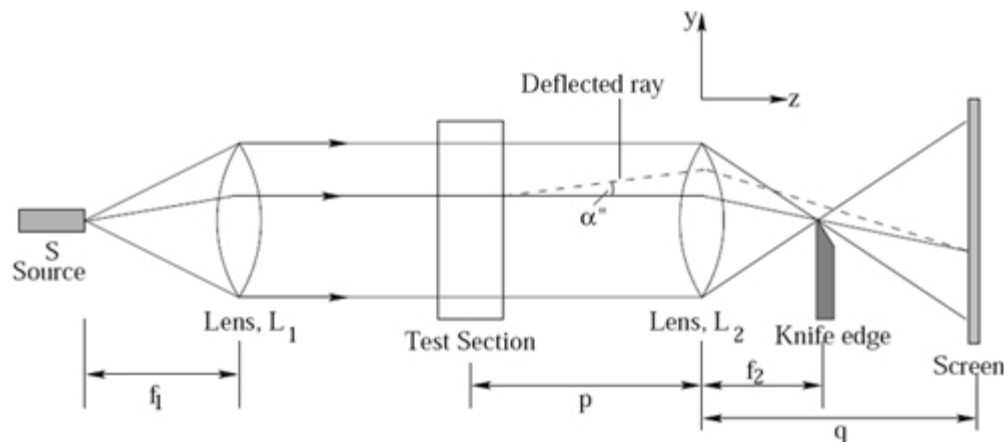

Figure 5.3: Schematic showing the path of light beam in a typical schlieren system

The dotted lines shows the path of the light beam in the presence of disturbances in the test region. The second lens L_2, kept at the focus of the knife-edge collects the light beam and passes onto the screen located at the conjugate focus of the test section.
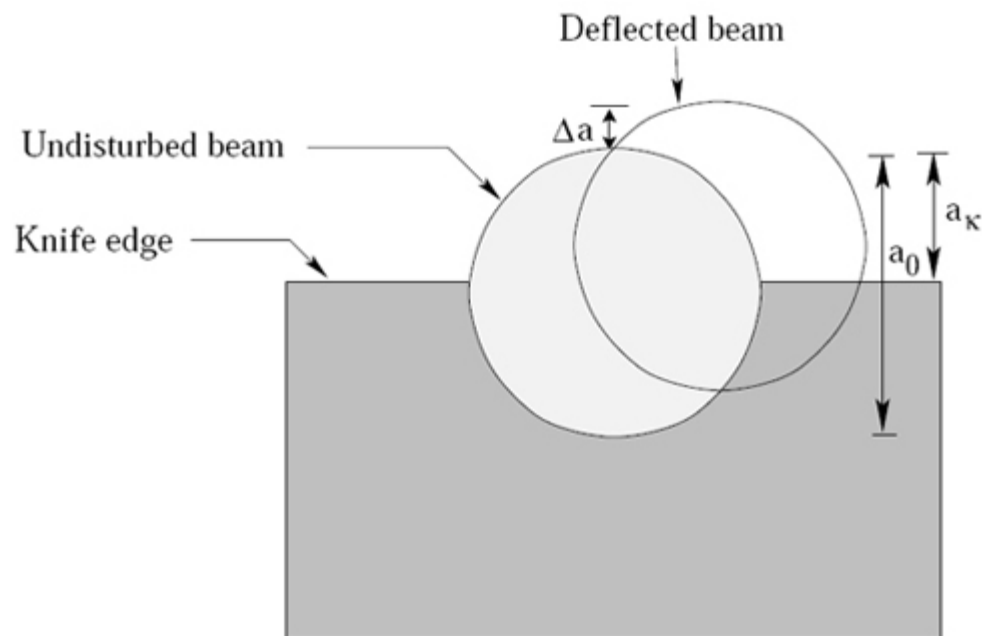
Figure 5.4: View of deflected and undistributed beams at the knife-edge of a schlieren system.

If no disturbance is present, the light beam at the focus of L_2 would be ideally as shown in Figure 5.4, with dimensions $a_0 \times b_0$. These are related to the initial dimensions by the formulas

$$\frac{a_0}{a_s} = \frac{b_0}{b_s} = \frac{f_2}{f_1}$$

where f_1 and f_2 are the focal lengths of L_1 and L_2, respectively.

In a schlieren system, the knife edge kept at the focal length of the second concave mirror is first adjusted, when no disturbance in the test region is present, to cut off all but an amount correnponding to the dimension a_k of the light beam Let a_0 be the original size of the laser beam. If the knife edge is properly positioned, the illumination at the screen uniformaly changes depending upon its direction of the movement. Let I_0 be the be the illumination at the screen when no knife-edge is present. The illumination I_k with the knife-edge inserted in the focal plane of the of the second concave mirror but without any disturbance in the test region will be given by

$$I_k = \frac{a_k}{a_0} I_0 \tag{4}$$

Let Δa be the deflection of the light beam in the vertical direction (y) above the knife edge corresponding to the angular deflection $(\alpha")$ of the beam after the test region experiences a change in the refractive index. Then from Figure 5.4, Δa can be expressed as

$$\Delta a = \pm f_2 \, \alpha" \tag{5}$$

where the sign is determined by the direction of the displacement of the laser beam in the vertical direction; it is positive when the shift is in the upward direction and negative if the laser beam gets

deflected below the level of the knife-edge. In the present discussion, the gradients in the fluid layer are in the upward direction and only the positive sign in Equation 5 is considered.

Contd...

Let I_f be the final; illumination on the screen after the light beam has deflected upwards by an amount Δa due to the inhomogeneous distribution of refractive index gradients in the test cell. Hence

$$I_f = I_k \frac{a_k + \Delta a}{a_k} = I_k \left(1 + \frac{\Delta a}{a_k}\right) \qquad (6)$$

The change in the light intensity on the screen ΔI is given by

$$\Delta I = I_f - I_k$$

The relative intensity or contrast can be expressed as

$$contrast = \frac{\Delta I}{I_k} = \frac{I_f - I_k}{I_k} = \frac{\Delta a}{a_k} \qquad (7)$$

Using Equation 5

$$contrast = \frac{a'' f_2}{a_k} = \frac{\Delta I}{I_k} \qquad (8)$$

Equation 8 shows that the contrast in a schlieren system is directly proportional to the focal length of the second lens. Larger the focal length, greater will be the sensitivity of the system.

Combining Equations 3 and 8

$$\frac{\Delta I}{I_k} = \frac{f_2}{a_k} \int_0^L \frac{\partial n}{\partial y} \, dz \qquad (9)$$

This equation shows that the schlieren technique records the average gradient of refractive index over the path of the light beam. If the field is two dimensional with the refractive index gradient $(\partial n / \partial y)$ constant at a given $x - y$ position over the length L in the z direction, then

$$\frac{\Delta I}{I_k} = \frac{f_2}{a_k} \frac{\partial n}{\partial y} L \qquad (10)$$

Equation 10 holds for every position in the test section and gives the contrast at the equivalent position in the image on the screen. The quantity on the left hand side can be obtained by using the initial and final inensity distribution on the screen. L is the length of the test section along the direction of the propogation of the laser beam, f_2 is the focal length of the second concave mirror and a_k is the size of the focal spot at the knife-edge. Usually, the knife-edge is adjusted in such a position that it cuts off approxiamtely 50% of the original light intensity, i.e. $a_k = a_0/2$ where a_0 is the original dimension of the laser beam at the pin-hole of the spatial filter. Typically, for a He-Ne laser (employed as the light source in the present work) a_0 is of the order of 10-100 microns. With $a_k = a_0/2$ Equation 10 can be written as

$$\frac{\Delta I}{I_k} = \frac{2 f_2}{a_0} \frac{\partial n}{\partial y} L \qquad (11)$$

Equation 11 represents the governing equation for the schlieren process in terms of the ray-averaged refractive index. It requires the approximation that changes in the light intensity occur due to beam deflection, rather than its physical displacement.

If the working fluid is a gas (e.g. air as employed in the validation experiments of the present study), the first derivative of the refractive index field with respect to y can be expressed as

$$\frac{\partial \rho}{\partial y} = \frac{\rho_0}{n_0 - 1} \frac{\partial n}{\partial y} \qquad (12)$$

Equation 12 relates the gradient in the refractive index field with the gradients of the density field with the gradients of the density field in the fluid medium inside the test cell. The governing equation for the schlieren process in gas (Equation 11) can be rewritten as

$$\frac{\Delta I}{I_k} = \frac{f_2}{a_k} \frac{n_0 - 1}{\rho_0} \frac{\partial \rho}{\partial y} L \qquad (13)$$

Assuming that pressure inside the test cell is practically constant, we get

$$\frac{\Delta I}{I_k} = -\frac{f_2}{a_k} \frac{n_0 - 1}{\rho_0} \frac{\rho}{RT^2} \frac{\partial T}{\partial y} L \qquad (14)$$

Equation 13 and 14 respectively relate the contrast measured using a laser schlieren technique with the density and temperature gradients in the test section. With the value of the dependent variables defined in the bulk of the fluid medium or with proper boundary conditions, the above equations can be solved to determine the quantity of interest.

For a growing KDP crystal, the refractive-index field gradients of the KDP solution and the concentration gradients are related using the following formula:

$$\frac{\partial N}{\partial y} = \frac{9n}{2\alpha_{KDP} \ (n^2 + 2)^2} \frac{\partial n}{\partial y}$$

(15)

Here α_{KDP} is the polarizability of the KDP $crystal \ (= 4.0 \ cm^3/mole)$ and N is the molar concentration of the solution (moles per 100 gram of the solution). Combining Equations 9 and 15 and integrating from a location in the bulk of the solution (where the gradients are negligible) , the concentration distribution around the growing crystal can be uniquely determined. Equations 13 and 14 show that the schlieren measurements are primamarily based on the original intensity distribution as recorded by the CCD camera. Though the schlieren images shown in the present work for qualitative interpretation of the fluids region have been subjected to image processing operations for contrast enhancement, original images as recorded by the CCD camera are employed for quantitative analysis. Figure 5.5 shows a set of four consecutive schlieren images and their averaged image. The images show a convective plume in the form of high intensity regions above a crystal growing from its aqueous solution and are discussed in detail in the subsequent lectures (27-33).
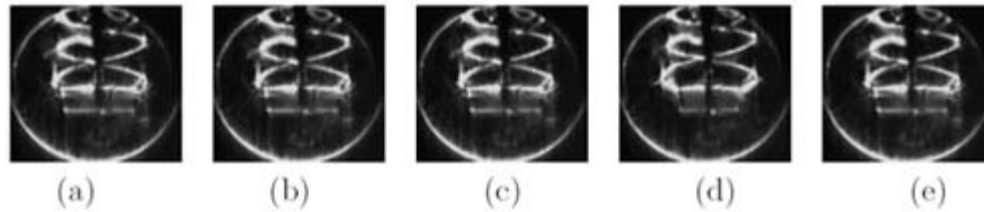
(a)   (b)   (c)   (d)   (e)

Figure 5.5: Original schlieren images (a-d) of convective field as recorded by the CCD camera and the corresponding time-averaged image(e).

◀|||Previous   Next |||▶

Window Correction

For visualization of the concentration field by the schlieren technique, circular optical windows have been fixed on the walls of the growth chamber at opposite ends. THe optical window employed in the present discussion of crystal growth is of finite thickness (5 mm) and the index of refraction of its material (BK-7) is considerably different from that of a KDP solution and air. The light beam emerging out of the KDP solution with an angular deflection α'' due to the variable concentration gradients in the growth chamber again undergoes refraction before finally emerging into the surrounding environment. The contribution of refraction of light at the confining optical windows can be accounted for by applying a correction factor in Equation 11 as discussed below.

The laser beam strikes the second optical window fixed on the growth chamber at an angle after undergoing refraction due to variable concentration gradients in the vicinity of the growing KDP crystal. The optical windows are made of BK-7 material with index of refraction $(n_{windows})$ equal to 1.509. The refractive index of the KDP solution at an average temperature of $30°C$ (n_{KDP}) is equal to 1.355 and for air $n_{air} = 1.00$. Let α'' be the angular deflection of the beam purely due to the presence of concentration gradients in the vicinity of the growing crystal as shown schematically in Figure 5.6.
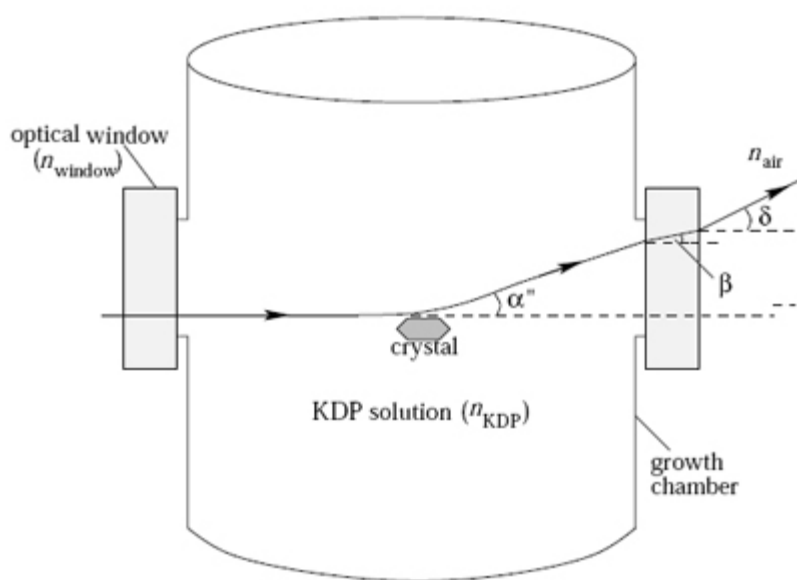

Figure 5.6: Schematic drawing showing the path of the light beam and the corresponding angles of deflection as it passes through the growth chamber. (Dimension in the figure are exaggerated for clarity).

The beam strikes the second optical window at this angle. Let β be the angle at which the laser beam emerges out of the second optical window. The angle at which the laser beam emerges out of the second optical window can be determined in terms of α'' using Snell's law as

$$\frac{n_{KDP}}{n_{window}} = \frac{sin\beta}{sin\alpha''} \qquad (16)$$

◀|||**Previous**   **Next**|||▶

Contd...

Since α'' is quite small, $\sin\alpha'' \approx \alpha''$, and

$$\sin\beta = \left(\frac{n_{KDP}}{n_{windows}}\right)\alpha'' \tag{17}$$

Let δ be the final angle of refraction with which the laser beam emerges into the surrounding air. For the optical window-air combination,

$$\frac{n_{windows}}{n_{air}} = \frac{\sin\delta}{\sin\beta} \tag{18}$$

Substituting the value of $\sin\beta$ from Equation 17 into Equation 18, the angle with which the laser beam emerges into the surrounding medium can be expressed as

$$\sin\delta = \left(\frac{n_{windows}}{n_{air}}\right)\left(\frac{n_{KDP}}{n_{window}}\right)\alpha'' \tag{19}$$

or

$$\sin\delta \approx \delta = \left(\frac{n_{KDP}}{n_{air}}\right)\alpha'' \tag{20}$$

Since $n_{air} = 1.00$,

$$\delta = (n_{KDP})\alpha'' = 1.355\alpha'' \tag{21}$$

Hence a correction factor equal to the refractive index of the KDP solution at the ambient temperature is taken into consideration for calculating the angle at which the laser beam emerges into the surrounding medium.

◀◀ **Previous**   **Next** ▶▶

Shadowgraph

The shadowgraph arrangement depends on the change in the light intensity arising from beam displacement from its original path. When passing through the test field under investigation, the individual light rays are refracted and bent out of their original path. The rays traversing the region that has no gradient are not deflected, whereas the rays traversing the region that has non zero gradients are bent up. Figure 5.7 illustrates the shadowgraph effect using simple geometric ray tracing. Here a plane wave traverses a medium that has a nonuniform index of refraction distribution and is allowed to illuminate a screen. The resulting image on the screen consists of regions where the rays converege and diverge; these appear as light and dark regions respectively. It is this effect that gives the technique its name because gradients leave a shadow, or dark region, on the viewing screen. A particular deflected light ray that arrives at a point different from the original point of the recording plane should be traced. It leads to a distribution of light intensity in that plane altered with respect to the undistributed case.

When subjected to linear approximations that includes small displacement of the light ray, a second order partial differential equation can be derived for the refractive index feild with respect to intensity contrast in the shadowgraph image. Let D be the distance of the screen from the optical window on the beaker. The governing equation for a shadowgraph process can be expressed as

$$\frac{\Delta I}{I_0} = D \int \left(\frac{\partial^2}{\partial x^2} + \frac{\partial^2}{\partial y^2} \right) (\ln n) \, dz \qquad\qquad (22)$$
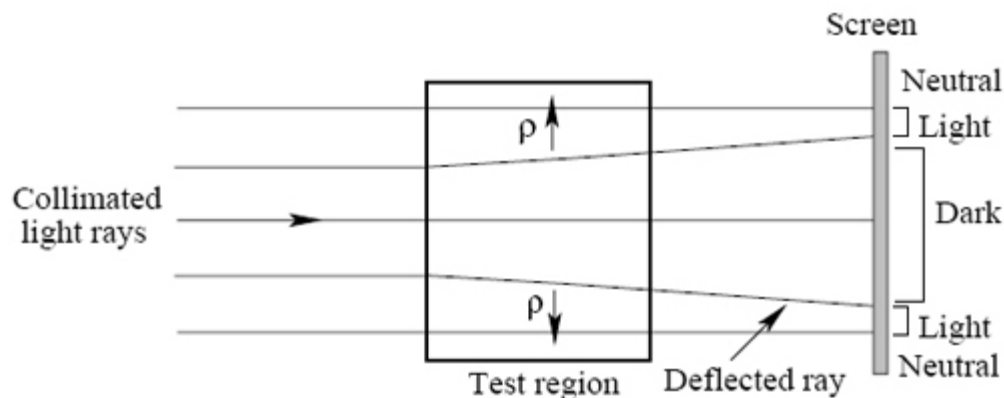

Figure 5.7: Illustration of the shadowgraph arrangement

Previous   Next

Contd...

Here ΔI is the change in illumination on the screen due to the beam displacement from its original path and I_0 is the original intensity distribution. Equation 22 implies that the shadowgraph is sensitive to changes in the second derivative of the refractive index along the line of sight of the of the light beam in the fluid medium. Integration of the Poisson equation (22) can be performed by a numerical technique, say the method of finite differences.

From Equation 22 it is evident that the shadowgraph is not a suitable method for quantitative measurement of the fluid density, since such an evaluation requires one to perform a double integration of the data. However, owing to its simplicity the shadowgraph is a convenient method for obtaining a quick survey of flow fields with varying fluid density. When the approximations involved in Equation 22 do not apply, shadowgraph can be used for flow visualization alone.

The present lecture has a discussion on how shadowgraph images can be analyzed to retrieve information on the concentration field.

Shadowgraphy

It employs an expanded and collimated beam of laser light. The light beam traverses the field of disturbance, an aqueous solution of KDP in the present application. If the disturbance is a field of varying refractive index, the individual light rays passing through the field are refracted and bent out of their original path. This causes a spatial modulation of the light intensity distribution. The resulting pattern is a shadow of the refractive-index field in the region of the disturbance.

Governing equation and Approximations

Consider a medium with refractive index n that depends on all the three space coordinates, namely $n = n\,(x, y, z)$. We are interested in tracing the path of light rays as they pass through this medium. Starting with the knowledge of the angle and the point of incidence of the ray at the entrance plane, we would like to know the location of the exit point on the exit window, and the curvature of the emergent ray.

Let the ray be incident at point $P_i = (x_i,\ y_i,\ z_i)$ and the exit point be $P_e = (x_e,\ y_e,\ z_e)$. According to Fermat's principle the optical path length traversed by the light beam between these two points has to be an extremum. If the geometric path length is L, then the optical path length is given by the product of the geometric path length with the refractive index of the medium. Thus

$$\delta \left(\int_{P_i}^{P_e} n(x,y,z)\,ds \right) \tag{23}$$

◀◀◀ Previous   Next ▶▶▶

Parameterizing the light path by z, the condition (Equation 23) can be represented by two functions $x(z)$ and $y(z)$, and the equation can be written as

$$\delta \left(\int_{z_i}^{z_e} n(x, y, z) \sqrt{x'^2 + y'^2 + 1}\, dz \right) \qquad (24)$$

where the primes denote differentiation with respect to z. Application of the variational principle to the above equation yields two coupled Euler-Lagrange equations, that can be written in the form of the following differential equations for $x(z)$ and $y(z)$:

$$x''(z) = \frac{1}{n}(1 + x'^2 + y'^2)\left(\frac{\partial n}{\partial x} - x'\frac{\partial n}{\partial z}\right) \qquad (25)$$

$$y''(z) = \frac{1}{n}(1 + x'^2 + y'^2)\left(\frac{\partial n}{\partial x} - y'\frac{\partial n}{\partial z}\right) \qquad (26)$$

The four constants of integration required to solve these equations comes from the boundary conditions at the entry plane of the chamber. These are the co-ordinates $x_i = x(z_i), y_i = y(z_i)$ of the entry point z_i and the local derivatives $x_i' = x'(z_i), y_i' = y'(z_i)$. The solution of the above equation yields the two orthogonal components of the deflection of the ray at the exit plane, and also its gradient on exit.

In the experiments performed, the medium has been confined between parallel planes and the illumination is via a parallel beam perpendicular to the entry plane. The length of the growth chamber containing the fluid is D and the screen is at a distance L behind the growth chamber. The $z-$ coordinates at entry, exit and on the screen are given by z_i, z_e and z_s respectively. Since the incident beam is normal to the entrance plane, there is no refraction at the optical window. Hence the derivatives of all the incoming light rays at the entry plane are zero; $x_i' = y_i' = 0$. The displacements $(x_s - x_i)$ and $(y_s - y_i)$ of the light ray on the screen (x_s, y_s) with respect to its entry position (x_i, y_i) are

$$(x_s - x_i) = (x_e - x_i) + Lx'(z_e) \qquad (27)$$

$$(y_s - y_i) = (y_e - y_i) + Ly'(z_e) \qquad (28)$$

where x_e, y_e and $x'(z_e), y'(z_e)$ are given by the solutions of previous equations at z_e.

The above formulation can be further simplified with the following assumptions.

◀|||Previous   Next|||▶

Assumption 1. Assume that the light rays incident normally at the entrance plane undergo only infinitesimal deviations inside the inhomogeneous field, but have a finite curvature on exiting the chamber. The derivatives $x'(z_e)$ and $y'(z_e)$ at the exit plane have finite values. The assumption is justifiable because of the smoothly varying refractive index in a fluid medium. Under this assumption Equations25 and 28 become

$$x''(z) = \frac{1}{n}\left(\frac{\partial n}{\partial x}\right) \tag{30}$$

$$y''(z) = \frac{1}{n}\left(\frac{\partial n}{\partial y}\right) \tag{31}$$

$$x_s - x_i = Lx'(z_e) \tag{32}$$

$$y_s - y_i = Ly'(z_e) \tag{33}$$

Rewriting the Equations 32 and 33 as

$$x_s - x_i = L\int_{z_i}^{z_e} x''(z)\,dz \tag{34}$$

$$y_s - y_i = L\int_{z_i}^{z_e} y''(z)\,dz, \tag{35}$$

and using Equations 30 and 31, Equations 34 and 35 become

$$x_s - x_i = L\int_{z_i}^{z_e} \frac{\partial(\log n)}{\partial x}\,dz \tag{36}$$

$$y_s - y_i = L\int_{z_i}^{z_e} \frac{\partial(\log n)}{\partial y}\,dz \tag{37}$$

◀|||Previous   Next|||▶

Assumption 2 : The assumption of the infinitesimal displacement inside the growth chamber can be extended and taken to be valid even for the region falling between the screen and the exit plane of the chamber. As a result, the coordinates of the ray on the screen can be written as

$$x_s = x_i + \delta_x(x_i, y_i) \tag{38}$$

$$y_s = y_i + \delta_y(x_i, y_i) \tag{39}$$

The deviation of the rays from their original paths in occurs through the inhomogeneous medium. In the absence of the inhomogeneous field, such an area is a regular quadrilateral. It transforms to a deformed quadrilateral when imaged on to a screen in the presence of the inhomogeneous field. The summation in the above equation extends over all the rays passing through points (x_i, y_i) at the entry of the test section that are mapped onto the small quadrilateral (x_s, y_s) on the screen. Considering the fact that the area of the initial spread of the light beam gets deformed on passing through the refractive medium, the intensity at point (x_s, y_s) is

$$I_s(x_s, y_s) = \sum_{(x_i, y_i)} \frac{I_o(x_i, y_i)}{\left|\dfrac{\partial(x_s, y_s)}{\partial(x_i, y_i)}\right|} \tag{40}$$

where I_s is the intensity on the screen in the presence of the inhomogeneous refractive index field, and I_o is the original undisturbed intensity distribution. The denominator in the above equation is the Jacobian $J(x_i, y_i, x_s, y_s)$ of the mapping function of (x_i, y_i) onto (x_s, y_s) as shown in Ffigure 5.8.
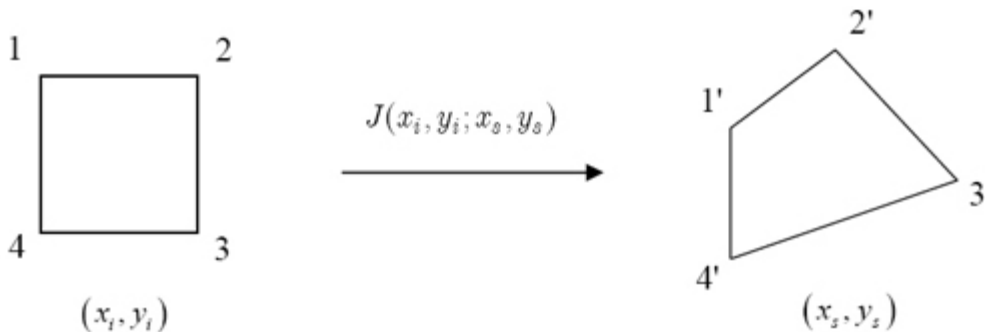

Figure 5.8: Jacobian $J(x_i, y_i, x_s, y_s)$ of the mapping function (x_i, y_i) onto (x_s, y_s)

Geometrically it represents the ratio of the area enclosed by four adjacent rays after and before passing through the inhomogeneous medium. In the absence of the inhomogeneous field, such an area is a regular quadrilateral. It transforms to a deformed quadrilateral when imaged on to a screen in the presence of the inhomogeneous field. The summation in the above equation extends over all the rays passing through points (x_i, y_i) at the entry of the test section that are mapped onto the small quadrilateral (x_s, y_s) on the screen and contribute to the light intensity within.

Assumption 3: Under the assumption of infinitesimal displacements, the deflections δ_x and δ_y are small. Therefore the Jacobian can be assumed to be linearly dependent on them by neglecting the higher powers of δ_x and δ_y, and also their product. Therefore, the jacobian can be expressed as

$$\left| \frac{\partial (x_s, y_s)}{\partial (x_i, y_z)} \right| \approx 1 + \frac{\partial (x_s - x_i)}{\partial x} + \frac{\partial (y_s - y_i)}{\partial y} \qquad (41)$$

Substituting in Equation 39, we get

$$I_s(x_s, y_s) \left[1 + \frac{\partial (x_s - x_i)}{\partial x} + \frac{\partial (y_s - y_i)}{\partial y} \right] = \sum_{(x_i, y_i)} I_o(x_i, y_i) \qquad (42)$$

Simplifying further we get

$$\frac{I_o(x_i, y_i) - I_s(x_s, y_s)}{I_s(x_s, y_s)} = \frac{\partial (x_s - x_i)}{\partial x} + \frac{\partial (y_s - y_i)}{\partial y} \qquad (43)$$

Using Equations 36 and 37 for $(x_s - x_i)$ and $(y_s - y_i)$, and integrating over the dimensions of the growth chamber, we get

$$\frac{I_o(x_i, y_i) - I_s(x_s, y_s)}{I_s(x_s, y_s)} = (L \times D) \left(\frac{\partial^2}{\partial x^2} + \frac{\partial^2}{\partial y^2} \right) \{ \log n(x.y) \} \qquad (44)$$

Equation 44 is the governing equation of the shadowgraph process under the set of linearizing approximation 1-3. In concise from the above equation can be rewritten as

$$\frac{I_o - I_s}{I_s} = (L \times D) \nabla^2 \{ \log n(x, y) \} \qquad (45)$$

◀|| Previous   Next ||▶

Numerical Solution of the Poisson Equation

The governing equation of the shadowgraph process (Equation 44) relates the intensity variation in the shadowgraph image to the refractive index field of the inhomogeneous medium. In order to solve the equation to obtain the refractive index, the following numerical procedure is adopted. First, the Poisson equation is discretized over the physical domain of interest by a finite-difference method. The resulting system of algebraic equations is solved for the image under consideration to yield a depth averaged refractive index value for each node point of the grid. A mix of Dirichlet and Neumann boundary conditions are used for the purpose. The refractive index conditions typically used on the boundaries of a crystal growth chamber are shown inn Figure 5.9. A computer code can be written for solving the Poisson equation, and it can be validated against analytical examples.
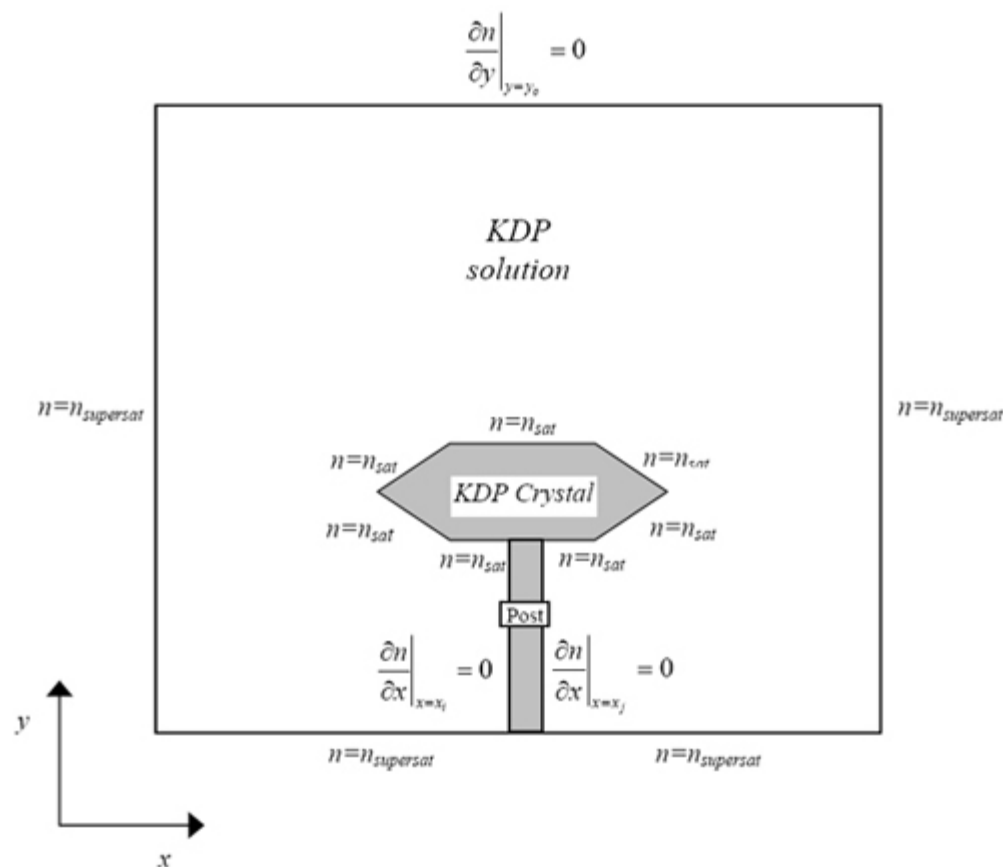

Figure 5.9: Refractive index specification on the boundaries.

The experimental input to the code is in the form of a matrix containing the gray value of each pixel of the shadowgraph image. The output generated by the Poisson solver is a matrix containing the averaged refractive index at each node point of the grid. Since the relationship between thee refractive index and the concentration of the KDP saturated solution at different temperatures is well documented, the refractive indices can be related to concentration over every frame of the image record.

Ray tracing through the fluid medium: Importance of the higher-order effects

In order to assess the importance of higher-order optical effects in shadowgraph imaging, the extent of the bending of rays is estimated by tracing the passage of rays through the fluid phase. In order to be able to do this, the shadowgraph images of the growth process recorded at different stages of growth are analyzed as follows: The Poisson equation governing the shadowgraph process is solved numerically to yield a depth-averaged refractive index value for each node point of the grid. The refractive index information is then used to determine the deflection of the ray at the exit plane of the growth chamber by solving the coupled ordinary differential equations (ODEs) governing the passage of light ray through the region of disturbance. The solution of these equation yields the two orthogonal components of the deflection of the ray and its gradient at the exit plane of the test cell. For the Poisson equation to be applicable for shadowgraph analysis, the ray deflections should be small.

Considering the length of the growth chamber containing the fluid as D and the screen to be at a distance L behind the test section, the displacements $(x_s - x_i) \ and \ (y_s - y_i)$ of a light ray on the screen with respect to its entry position are given by Equations 27 and 28. A computer code for solving the coupled ODEs has been written and validated against analytical examples.

Correction factor for refraction at the glass-air interface

In order to perform laser shadowgraphic and interferometric imaging of the crystal growth process, two different growth chambers were fabricated. The crystal growth process referred here is described in detail in lectures 27-33. The growth chambers have optical windows for the entry and exit of the laser beam. The cavity is enclosed between the windows for the entry and exit of the laser beam. The cavity enclosed between the windows was filled with the KDP solution. During the process of crystal growth the KDP solution is a medium of varying refractive index, leading to the bending of the rays as the laser beam traverses through the solution. At the exit from the growth chamber, the light ray encounters two different interfaces, namely KDP-solution and glass, followed by glass and air. Thus, the light ray emerges at an angle different from the angle at which it is incident on the solution and glass interface. The refractive indices of the KDP solution, the quartz window and the air around result in a scale factor which must be taken into account to get the correct emergent angle of ray. The optical path of the light ray through the two interfaces is shown in Figure 5.10.
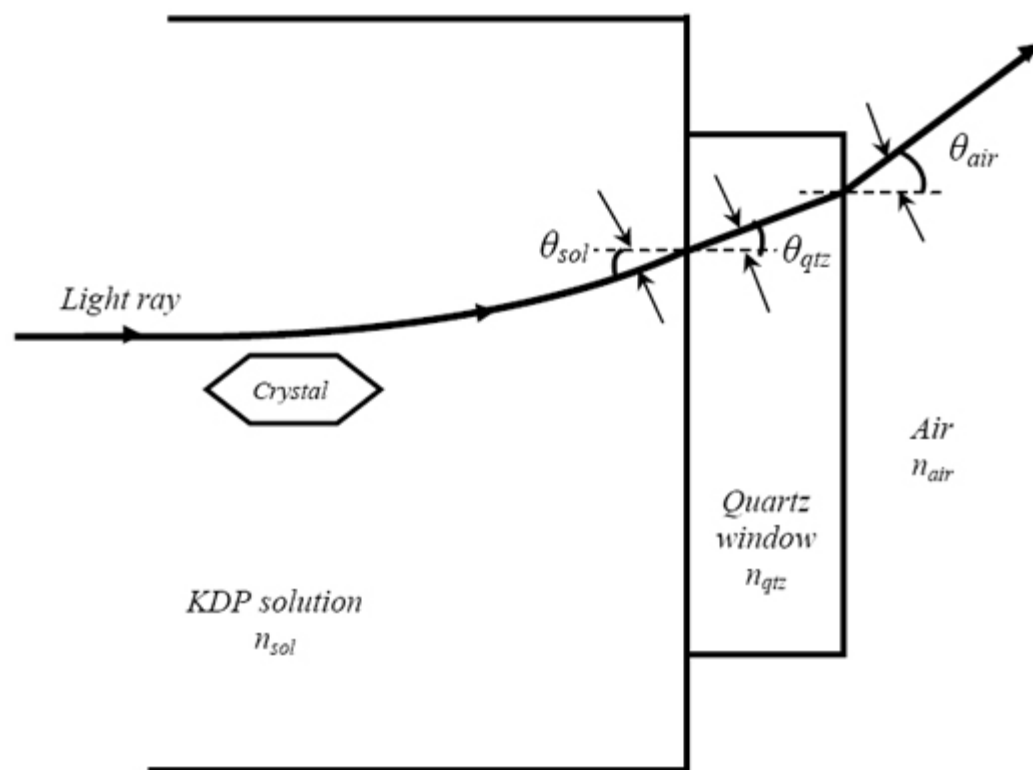
Figure 5.10: Optical Path of the light ray passing from the growth chamber into the air.

Previous   Next

Contd...

The scale factor used in calculations is derived below.

Applying Snell's law for refraction of the light ray passing from the KDP-solution into the quartz optical window, we get

$$\frac{\sin \theta_{sol}}{\sin \theta_{qtz}} = \frac{n_{qtz}}{n_{sol}} \tag{46}$$

where $\theta_{sol}, \theta_{qtz}, n_{sol}$ and n_{qtz} are the angles of incidences of the light at the quartz window, the angle of refraction of the light ray into the quartz window, the refractive index of the KDP solution, and the refractive index of the quartz window respectively. Applying Snell's law again for the ray passing from the quartz optical window to the surrounding air, we get

$$\frac{\sin \theta_{qtz}}{\sin \theta_{air}} = \frac{n_{air}}{n_{qtz}} \tag{47}$$

where $\theta_{qtz}, \theta_{air}, n_{qtz}$ and n_{air} are the angles of refraction of the light ray into the quartz window, the angle of refection of the light ray in the air, the refractive index of the quartz window, and the refractive index of air respectively. Substituting the expression for $\sin \theta_{qtz}$ from Equation 46 into Equation 47, we get

$$\frac{\sin \theta_{sol}}{\sin \theta_{air}} = \frac{n_{air}}{n_{sol}}$$

Under the small-angle approximation $\sin \theta \approx \theta$, and

$$\frac{\theta_{sol}}{\theta_{air}} \approx \frac{n_{air}}{n_{sol}}$$

Hence

$$\theta_{air} \approx \frac{n_{sol}}{n_{air}} \theta_{sol} \tag{48}$$

Thus the correction factor for additional refraction at the optical windows is $\frac{n_{sol}}{n_{air}}$.

◀‖ Previous   Next ‖▶